

Versatile Digital GHz Phase Lock for External Cavity Diode Lasers

Jürgen Appel*

Niels Bohr Institute, Copenhagen University, 2100 København, Denmark

Andrew MacRae[†] and A. I. Lvovsky[‡]

Institute for Quantum Information Science, University of Calgary, Alberta T2N 1N4, Canada

(Dated: November 26, 2024)

We present a versatile, inexpensive and simple optical phase lock for applications in atomic physics experiments. Thanks to all-digital phase detection and implementation of beat frequency pre-scaling, the apparatus requires no microwave-range reference input, and permits phase locking at frequency differences ranging from sub-MHz to 7 GHz (and with minor extension, to 12 GHz). The locking range thus covers ground state hyperfine splittings of all alkali metals, which makes this system a universal tool for many experiments on coherent interaction between light and atoms.

PACS numbers: 42.60.-v, 85.6.Bf, 07.60.-j

INTRODUCTION

Many experiments on coherent interaction of light with matter require two or more separate light fields whose frequency difference is precisely maintained at a particular value. If the required frequency difference is relatively small, the mutually coherent fields can be produced by splitting the light from a single source and shifting the frequency by acousto-optic or electro-optic modulation. But if the frequencies of the required fields differ by more than a few hundred MHz, frequency modulation techniques become impractical and it is often preferable to use two separate sources. In this case, long-term phase coherence between these sources can be achieved using an optical phase locked loop (OPLL). In such an OPLL, the rate at which the relative phase between a master laser and a slave laser changes is locked to a fixed value f_{beat} called the beat frequency.

A number of OPLL designs have been implemented [1–5]. However, most of the existing schemes are designed with a specific setup in mind and require expertise in microwave frequency electronics. Furthermore, these schemes require expensive equipment for the generation of stable microwave-range reference signals. In addition, the range of lockable beat frequencies is often restricted to less than an octave and a change in the experimental configuration requires major modifications in the hardware.

In this work, we present a versatile OPLL for use with external cavity diode lasers (ECDLs) which is simple to construct and is made from inexpensive off-the-shelf components. Recent advances in digital phase detection, associated with the development of wireless communications, allow us to develop a robust design which is insensitive to beat signal amplitudes over a wide range and avoids the frequency range limitations of passive microwave mixers. Since the beat frequency is divided down digitally, a versatile and inexpensive low frequency reference may be used. The high-frequency part of the printed

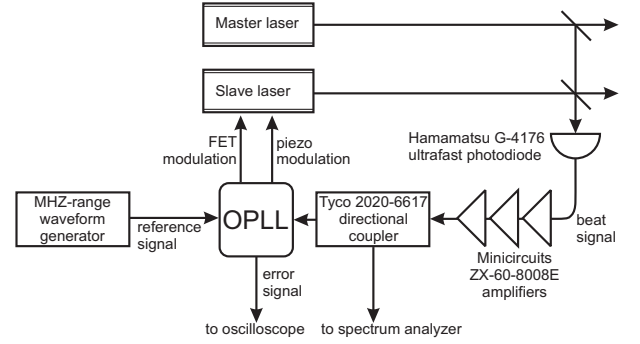


FIG. 1: Experimental setup implementing our phase lock.

circuit board layout is kept compact, so constructing the device does not require high frequency electronic measuring equipment and expertise.

In order to test the performance of the OPLL, the spectrum of the beat signal was measured around $f_{\text{beat}} = 6.9 \text{ GHz}$ and the phase variance $\langle(\Delta\phi)^2\rangle$ is found to be less than 0.08 rad^2 . Two lasers, each locked to the same source, were interfered and steady fringes were observed.

CONSTRUCTION OF THE DEVICE

The basic setup for our OPLL is displayed in figure 1. Beams from the master and slave lasers are mixed at a beam splitter and a total optical power of $0.5 - 2 \text{ mW}$ is focused onto a fast photodetector. The generated beat signal is amplified up to $\approx 0 \text{ dBm}$. A -10 dB directional coupler splits the beat frequency between a spectrum analyzer and the OPLL circuitry. Based on a reference signal received from a function generator, the OPLL produces the error signal for the slave laser, closing the feedback loop.

The coupler and the spectrum analyzer are not required for daily operation but prove to be useful to monitor lock performance when initially setting up the system.

Since the instantaneous bandwidth of a typical ECDL may span as much as a few hundreds of kilohertz, the loop must be made as fast as possible in order to correct for this noise. The loop must as well be able to correct for the low frequency noise and drifts due to mechanical vibrations. To achieve the required frequency range, dual feedback was employed: by modulating the external cavity length with a piezo-electric transducer, and by direct modulation of the injection current. The bandwidth of the piezo modulation is limited to a few kHz by mechanical resonances, but it allows significant correction to the laser frequency. On the other hand, the current injection modulation is fast (up to a few MHz), but the frequency corrections are limited by modehops.

The electric schematic of our OPLL is shown in figure 2. The reference and beat signals are sent into the digital phase-frequency-discriminator chip (*Analog devices ADF4107*). This chip divides the reference signal by a factor R and the beat signal by a factor N digitally and then compares frequency and phase of both divided signals with a dual flip-flop circuit. The ADF4107 is interfaced with a micro-controller that programs the divider quotients R and N on start-up and allows for easy change of these values. A similar circuit based on the ADF4007 that does not require programming but is less versatile has been constructed and shows similar performance.

The N counter can be programmed to any value between 24 and about 5×10^5 ; the range of permitted values of R can take values between 1 and 16,383. The phase lock can thus be implemented for the beat signal of any frequency up to the maximum permitted by the ADF4107 (7 GHz), with the reference produced by a generic MHz-range signal generator. When needed, the frequency range can be extended by preceding the OPLL beat signal input with a pre-divider (*Hittite HMC364S8G*). The lock stability generally improves with smaller values of N/R . It is particularly important that the divided reference frequency significantly exceed the required loop bandwidth.

If the phase difference of the beat and reference signals is small, this phase-frequency-discriminator circuit produces a feedback current proportional to this quantity. Otherwise the error signal polarity corresponds to the sign of the frequency difference between the two signals [6]. In this way, the capture range of the phase lock circuit is limited only by the mode hop free tuning range of the slave laser.

The feedback current enters a proportional-integral (PI) filter formed by C1, R9 and is amplified in two stages. Since the ADF4107's output voltage is restricted to a range of 0–5 V, a gain-two preamplifier (IC1A) converts the voltage on the PI Filter into a low impedance 0–10 V output. A negative 5 V bias is added so that the output of the second amplification stage (IC2) with gain 300 is symmetric around zero when locked. This bias

voltage has been strongly low pass filtered to avoid introducing noise to the error signal (using IC1B, not depicted in Fig. 2). Finally the output of IC2 is split into the fast and slow feedback paths.

A characteristic challenge in constructing a feedback circuit for a diode laser is due to the shape of its transfer function's phase. At low modulation frequencies, a change in the diode injection current affects the lasing frequency mainly because of the modulation of the recombination area's temperature. At high modulation frequencies, the lasing frequency is affected due to current induced charge density modulations which effect the refractive index of the gain medium. Unfortunately these two mechanisms oppose each other, which leads to a phase shift of 180° at modulation frequencies typically between 1–10 MHz [7]. In order to partly compensate for this effect, a phase-advance loop filter is used in the fast feedback path, followed by a buffer stage (IC1D) with an adjustable gain to drive the laser diode current modulator.

The current feedback is implemented as depicted in the inset in Fig. 2 and is based on the FET modulation circuit for Toptica DL100 lasers. The gate voltage of a N-junction field effect transistor is clamped by protection diodes. C13 approximately compensates the low-pass formed by the diodes' and the J-FET's capacitance. The input voltage causes the J-FET to bypass a fraction of the diode's supply current. This way the diode current never exceeds that provided by the current controller, so the expensive laser diode is protected.

We now describe the slow feedback path. The signal part is integrated by IC1C and R18, C8 to control the length of the external cavity. The integrator ensures that in the locked condition the output of stage IC2 is zero on average, so that the current modulation is free of DC components which may saturate the amplifier stages and drive the laser closer towards a mode-hop. A bipolar LED conveniently displays the integrator overrun, indicating the need for operator intervention.

The transfer function of the integrating arm controlling the piezo is not critical to the lock performance. In fact, we choose the gain in this path so high that, in the absence of the current feedback loop, oscillations about the target frequency occur. Once the fast current feedback is engaged it easily counters this effect and renders the loop stable as a whole.

Special care has been taken in order to obtain good noise performance. Since digital switching noise can have a detrimental effect on the operation, the analog and digital sections of the circuit each have their own voltage regulators and are located on separate ground planes.

This OPLL has been put in to operation in a variety of setups including locking a commercial Toptica DL-100 diode laser to a Coherent MBR Ti:Sapphire laser, a self made diode laser with an Eagleyard laser diode to the Ti:Sapphire laser, and two self-made diode lasers with

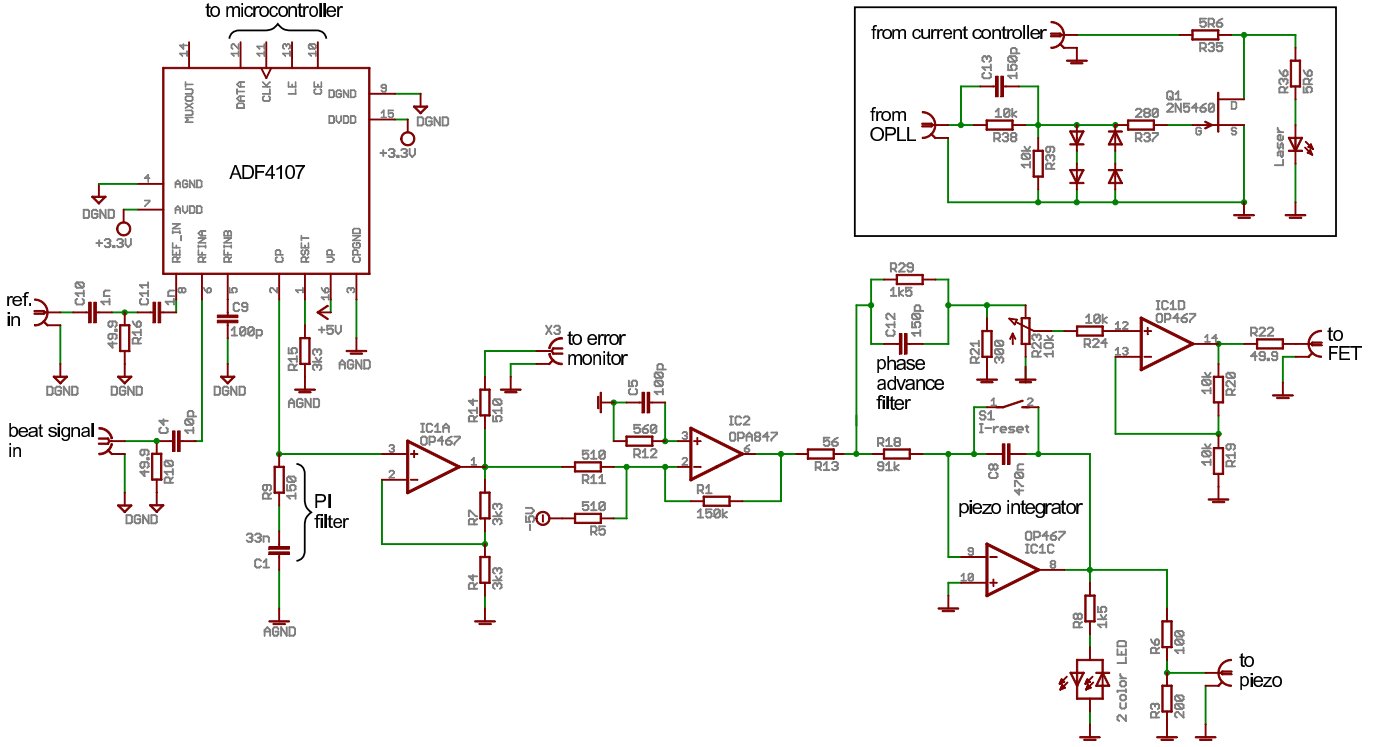


FIG. 2: Circuit diagram of the OPLL controller. Inset: Laser diode current modulator

Sharp and SDL diodes to each other.

CHARACTERIZATION OF LOCK PERFORMANCE

An important parameter for measuring the performance of a PLL is the mean-square phase error $\langle \Delta\phi^2 \rangle$. This error can be determined by measuring the power fraction of the carrier in the electronic spectrum $P(\nu)$ of the beat signal [2]:

$$\exp(-\langle \Delta\phi^2 \rangle) = \frac{P_{\text{carrier}}}{\int_{-\infty}^{\infty} P(\nu) d\nu}. \quad (1)$$

To that end we set up the lock circuit to operate at the frequency around 6.9 GHz and recorded the RF power spectrum in a 10 MHz frequency span around this frequency with a Hewlett-Packard E4405B spectrum analyzer. The spectrum analyzer resolution bandwidth was set to 3 kHz, video bandwidth to 30 kHz, and the detector type to *average* [8]. During a 100-s scan, the analyzer acquired a $n = 8192$ point data set. In this way, the resolution bandwidth is significantly larger than the frequency range associated with each data point (1.22 kHz).

The beat spectrum is shown in Fig. 3. Remarkably, the width of the central peak, corresponding to the carrier signal, could not be resolved even with the lowest

Reference	N	R	$ \Delta\phi ^2$
Agilent 33220A waveform generator at 18 MHz	384	1	0.19 rad ²
Agilent 33250A waveform generator at 72 MHz	96	1	0.33 rad ²
Mini-Circuits JTOS 400, phase locked to 216 MHz	96	3	0.08 rad ²

TABLE I: Phase noise

resolution bandwidth setting (10 Hz) of the spectrum analyzer.

The carrier power fraction is calculated from the acquired data set P_i (where $1 \leq i \leq n$) as follows. The power in the carrier P_{carrier} is the direct reading of the spectrum analyzer at the beat signal frequency. The surrounding noise power density $P(\nu)$ can be determined from P_i by applying the following corrections [9]. First, we add 2.51 dB to each P_i to compensate the error associated with the logarithmic scale envelope detection and subtract 0.52 dB to correct for the shape of the resolution bandwidth filter. Finally, by subtracting $10 \log_{10}(3000)$ dB, we normalize the noise power density to the 1-Hz bandwidth.

We performed the experiment with three reference oscillators, as summarized in Table I. The best results were obtained with a home-made generator consisting of a Mini-Circuits JTOS 400 voltage-controlled oscillator locked to an Agilent 33220A waveform generator using

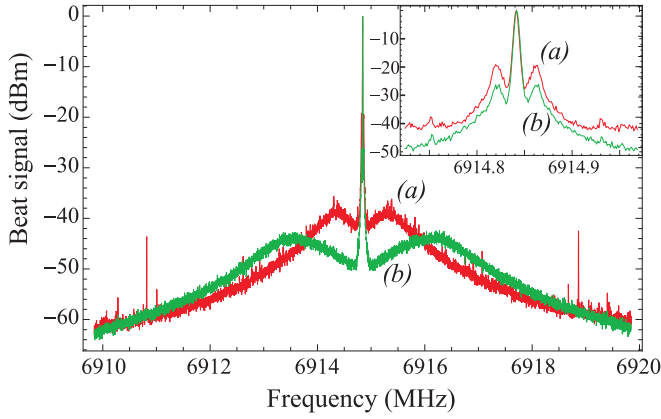


FIG. 3: Spectral noise density of the RF signal produced by interference of two phase locked lasers (Resolution bandwidth=3 kHz). Curve (a) is associated with a 18 MHz reference signal produced by an Agilent 33220A reference generator; curve (b) with a 216 MHz home-made generator. The inset shows a blowout of the central portion of the plot.

an additional, narrowband (~ 1 kHz) phase-lock circuit. The noise reduction associated with this generator is due to a low multiplication factor N/R . Note that in spite of a lower N , the lock with the Agilent 33250A reference generator (80 MHz) produces more noise than Agilent 33220A (20 MHz). We believe this to be due to the intrinsic phase noise of the reference signal, which is about -115 dBc/Hz for 33220A and -90 dBc/Hz for 33250A. These results emphasize the need for a low phase-noise reference oscillator with large N/R . Additionally a high phase detection frequency f_{beat}/N that is significantly bigger than the loop bandwidth is imperative to reduce the loop delay.

Ultimately even with a high quality reference oscillator the noise performance achievable with the direct digital phase locking approach presented in this work will be limited by the electronic noise floor of the phase-frequency-discriminator circuit ADF4107, which is given by -219 dBc/Hz $\times N \times f_{\text{beat}}/\text{Hz}$. Significantly lower values can be obtained circumventing the frequency division by multiplying up an ultra low noise frequency reference into the microwave regime and then using that to mix down the laser beat note signal. This however requires a much more complex and less versatile setup[5].

To illustrate the capabilities of our circuit, we have observed interference between two separate slave lasers, phase locked to the same master laser at 6.9 GHz and with a relative frequency difference of 3.84 Hz. The interference signal between the two slave lasers was measured with a fast photodiode and recorded with a digital oscilloscope. The result of this measurement is displayed in Fig. 4 and exhibits clearly discernible interference fringes.

Further insight into the noise behavior of the phase lock is provided by the modified Allan variance, which quantifies the average drift of the oscillator frequency

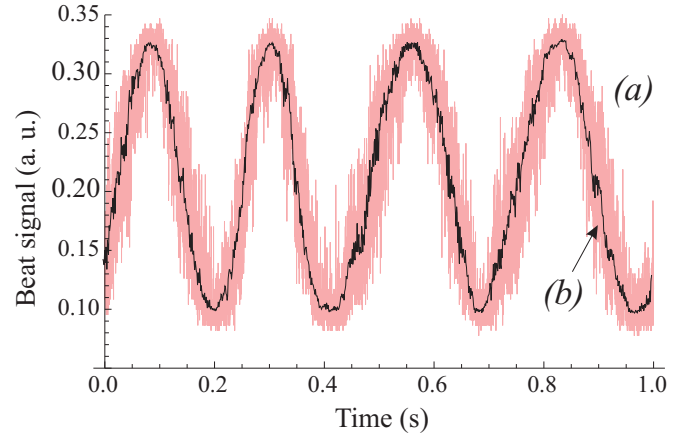


FIG. 4: 3.84-Hz beat signals between two slave lasers locked to the same master lasers, each with its own OPLL. Curve (a) represents a set of 1,000,000 data points; curve (b) the same set, smoothed by computing averages of 100-element bins.

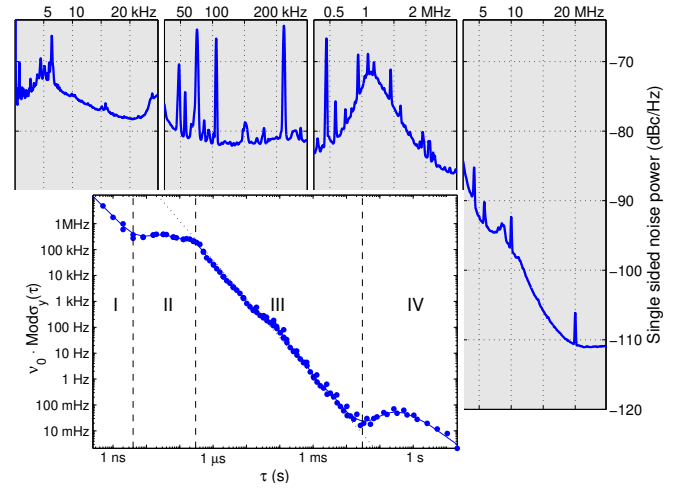


FIG. 5: **Background:** Power spectrum of the interference signal of two lasers phase locked to a common master. **Inset:** Modified Allan deviation based on the same signal. Roman numerals indicate regions of different dominating noise types, see text.

over time τ [10, 11]. Using the 10 MHz output of a digital oscilloscope as reference we phase locked two diode lasers to a common master laser at $f_{\text{beat}} = \nu_0 = 4$ GHz. To measure the Allan variance, we recorded four data sets of the interference signal between the slave lasers, with sampling rates ranging between 4×10^9 and 5×10^4 s $^{-1}$. For short acquisition times, via a slow (bandwidth < 1 Hz) feedback loop, a piezoelectric transducer varied the optical path lengths so that the interference pattern was held at 50% of its fringe. For acquisition times over 0.5s, the piezo signal was disengaged and the measurement was started manually after the pattern drifted to the 50% fringe position.

As depicted in the inset of Fig. 5, the modified Al-

lan deviation (root Allan variance) decreases approximately as $\tau^{-3/2}$ over a wide range of integration times between ~ 300 ns and ~ 30 ms (region III, black dotted line), which corresponds to uncorrelated white phase noise [11]. Shorter τ 's correspond to frequencies outside the free-running linewidth of the diode laser, so the Allan variance levels off ($1/f$ frequency noise, region II). At even shorter integration times (below ~ 10 ns, region I), the electronic noise of the photodetector comes into play, leading, again, to a behavior similar to white phase noise. At very large τ 's (region IV), the phase measurement is disturbed by optical path length fluctuations (vibrations, air flow), which show up as frequency and phase drifts.

The power spectrum of the interference signal of the two slave lasers is shown in Fig. 5. Below 10 kHz acoustic resonances are visible. At intermediate frequencies 50 kHz...1 MHz distinct narrow peaks corresponding to various electronic noise sources in the laboratory can be observed. At high frequencies the 10 MHz reference and a 4.7 MHz modulation which is used to modulate and lock the master laser can be identified. Increased noise at ≈ 1 MHz marks the loop bandwidth and indicates that the loop gain of at least one laser was chosen slightly too high. When sampling the phase difference signal of the two slaves with a rate of 5 MHz we find a root mean square phase variation of 0.05 rad^2 .

Phase and frequency stability is not the only important characteristics of a laser. For most of today's high precision measurements it is also important that the light intensity is stable to a high degree. Many quantum optics experiments rely on the property of diode lasers to emit light with intensity noise levels that are essentially shot noise limited at sideband frequencies over a few tens of kHz up to intensities of hundreds of microwatt. Since the phase lock circuit modulates the diode's injection current there is a potential risk in producing excess intensity noise when controlling the laser's phase. However we found the added intensity noise to be less than 3 dB/mW with respect to the shot noise level in a 500 kHz bandwidth. Since the laser diode current modulations mainly affect the frequency, a phase lock even quietens noisy current supplies to a certain degree.

CONCLUSION

In this paper, we have presented a simple, yet versatile optical phase lock operating in the frequency range from sub-MHz to 7 GHz. All-digital phase frequency detection leads to a wide capture range and renders the circuit robust against amplitude fluctuations of the beat signal. A special feature of this design is that the reference is provided by an affordable MHz-range waveform generator.

The unit contains virtually no microwave components, so it can be easily constructed with little experience in high frequency electronics.

Our circuit has been successfully tested in a number of different configurations and is an integral component of several experiments involving electromagnetically induced transparency in atomic ^{87}Rb , where the control and signal fields need to be phase locked to the ground state hyperfine splitting frequency (6.834 GHz) [12–16]. The high stability of the circuit permits long-duration measurements in atomic coherence experiments. Locking times of many days are routinely observed.

* Electronic address: jappel@nbi.dk

† Electronic address: amacrae@qis.ucalgary.ca

‡ Electronic address: lvov@ucalgary.ca

- [1] H. R. Telle, *Spectrochimica acta* **15**, 201 (1993).
- [2] T. H. M. Prevedelli, T. Freegarde, *Applied Physics B* **60**, 241 (1994).
- [3] L. Cacciapuoti, M. de Angelis, M. Fattori, G. Lamporesi, T. Petelski, M. Prevedelli, J. Stuhler, and G. M. Tino, *Review of Scientific Instruments* **76**, 053111 (2005).
- [4] A. M. Marino and J. C. R. Stroud, *Review of Scientific Instruments* **79**, 013104 (2008).
- [5] J. L. Gouët, T. Mehlstäubler, J. Kim, S. Merlet, A. Clairon, A. Landragin, and F. P. D. Santos, *Appl. Phys. B* **92**, 133 (2008).
- [6] M. Curtin and P. O'Brien, *Analog Dialogue* **33**, 9 (1999), *Phase-locked loops for high-frequency receivers and transmitters, Part I-III*.
- [7] S. Kobayashi, Y. Yamamoto, M. Ito, and T. Kimura, *IEEE Journal of Quantum Electronics* **18**, 582 (1982), ISSN 0018-9197.
- [8] *Spectrum Analyzer Basics (Application Note 150)*, Agilent Technologies (2008), URL http://www.home.agilent.com/upload/cmc_upload/All/5952-
- [9] *Spectrum Analyzer Measurements and Noise (Application Note 1303)*, Agilent Technologies (2008), URL <http://cp.literature.agilent.com/litweb/pdf/5966-4008E.>
- [10] D. Allan and J. Barnes, in *Proceedings of the 35th Annual Frequency Control Symposium* (Washington DC, 1981), 35, pp. 470–475.
- [11] J. Rutman and F. L. Walls, in *Proc. IEEE* (IEEE, 1991), vol. 79, pp. 952–960.
- [12] E. Figueroa, F. Vewinger, J. Appel, and A. I. Lvovsky, *Opt. Lett.* **31**, 2625 (2006).
- [13] F. Vewinger, J. Appel, E. Figueroa, and A. I. Lvovsky, *Opt. Lett.* **32**, 2771 (2007).
- [14] J. Appel, E. Figueroa, D. Korystov, M. Lobino, and A. I. Lvovsky, *Phys. Rev. Lett.* **100**, 093602 (2008).
- [15] E. Figueroa, M. Lobino, D. Korystov, J. Appel, and A. I. Lvovsky, arxiv:0804.2703 (2008).
- [16] A. MacRae, G. Campbell, and A. I. Lvovsky, *Opt. Lett.* **33**, 2659 (2008).